Boundary-Layer Meteorol (2011) 139:487–500
DOI 10.1007/s10546-011-9595-3

ARTICLE

Dispersion Coefficients for Gaussian Puff Models

Xiaoying Cao · Gilles Roy · William J. Hurley · William S. Andrews

Received: 21 May 2010 / Accepted: 24 January 2011 / Published online: 20 February 2011

Abstract The Gaussian distribution is a good approximation for transient (instantaneously released) puff concentration distributions within a short period of time after release. Artificial neural network (ANN) models for puff dispersion coefficients were developed, based on observations from field experiments covering a wide range of meteorological conditions (in March, May, August and November). Their average predictions were in very good agreement with measurements, having high correlation coefficients ($r > 0.99$). A non-linear multi-variable regression model for dispersion coefficients was also developed, under the assumption that puff dispersion coefficients increase with time, and follow power laws. Both ANN-based and multi-regression non-linear models were able to use easily measured atmospheric parameters directly, without the necessity of predefining the Pasquill stability category. Predictions of ANN-based and multi-regression-based Gaussian puff models were compared with those of Gaussian puff models using Slade's dispersion coefficients and COMBIC, a sophisticated model based on Gaussian distributions. Predictions from our two new models showed better agreement with concentration measurements than the other Gaussian puff models, by having a much higher fraction within a factor of two of measured values, and lower normalized mean square errors.

Keywords Artificial neural network · Gaussian puff model · Multi-variable regression · Puff dispersion coefficients

X. Cao · W. S. Andrews (✉)
Department of Chemistry and Chemical Engineering, Royal Military College of Canada, Kingston, ON K7K 7B4, Canada
e-mail: andrews-w@rmc.ca

G. Roy
Defence Research and Development Canada – Valcartier, Val-Belair, QC G3J 1X5, Canada

W. J. Hurley
Department of Business Administration, Royal Military College of Canada, Kingston, ON K7K 7B4, Canada

1 Introduction

Lagrangian stochastic (LS) particle models are usually accepted to be the most powerful tools for studying dispersion from passive non-buoyant releases (Wilson and Sawford 1996). To establish statistical significance, however, in the simulation of the dispersion of particles, a large number of particles (of the order of 10^5, according to De Hann and Rotach 1998; De Haan 1999) are typically required, with the concomitant requirement for computing resources. The concentration distribution of a transient (instantaneously released) puff, within a short time after release, can be approximated by a Gaussian shape (DeVito et al. 2009; Cao et al. 2010). Compared with LS particle models, Gaussian puff models are much simpler to use, and in operation take far less computer time. This is very important for a forward dispersion model used in a source inversion problem in emergency response operations to characterize the source location and strength. For Gaussian puff models, the key parameters are dispersion coefficients, which determine the effectiveness of the models. There is a variety of ways to estimate these coefficients. Equation 1 shows the most basic Gaussian puff model of concentration, c, for non-reactive passive dispersion with no deposition or reflection:

$$c(x, y, z, t) = \frac{Q}{(2\pi)^{3/2}\sigma_x\sigma_y\sigma_z} \exp\left\{-\frac{x^2}{2\sigma_x^2} - \frac{y^2}{2\sigma_y^2} - \frac{z^2}{2\sigma_z^2}\right\}, \tag{1}$$

where Q is the mass released at time $t = 0$, σ_x, σ_y and σ_z are dispersion coefficients in the downwind, crosswind and vertical directions, respectively, with the downwind direction taken as the x-axis, crosswind as the y-axis, and vertical as the z-axis, and x, y and z are relative distances to the centre of mass of the puff along each axis, at time t. When reflection from the ground surface is considered, Eq. 1 is then modified to add reflection terms.

In practice, the dispersion coefficients are often parametrized by a discrete atmospheric stability category, as well as the dispersion time t, or distance from the source. Unlike Gaussian plume models, whose dispersion coefficients are based on a significant amount of field measurements, the field data collection used to develop dispersion coefficients for Gaussian puff models has been very limited, due mainly to the challenges of measuring instantaneous concentration distributions. A number of models employ the parametrization scheme or modifications developed for plume spread. The validity of their use in puff models is questionable (Pasquill and Smith 1983; Arya 1999).

In the past, cameras were used to help determine the puff volume change, and in situ measurements of (integrated) concentration were used to analyse the puff concentration distribution. Islitzer and Slade (1968) summarized the earlier observations, and came up with power-law expressions for dispersion coefficients, as functions of Pasquill stability and distance from the point source. Slade's relations were based on far fewer observations than were the continuous plume relations of Pasquill stability (Turner 1994). Also, Slade did not develop a distinct expression for σ_x, as it was simply assumed that this longitudinal (downwind) dispersion coefficient would equal the lateral (crosswind) dispersion coefficient σ_y. According to Pasquill and Smith (1983), however, the downwind dispersion coefficient is larger than the lateral dispersion coefficient, due to the effects of wind shear. Further studies of puff dispersion show that downwind dispersion is a combined effect of vertical dispersion and wind shear (Chatwin 1968; Draxler 1979; Wilson 1981; Van Ulden 1992; Sato 1995).

In this study, artificial neural network (ANN) and multi-variable non-linear regression models were used to parametrize the dispersion coefficients of a puff model for a short dispersion time (less than 150 s). Easily measurable meteorological conditions and stability

parameters were used to derive the ANN models. This is the first attempt to use neural networks to address the parametrizations of Gaussian puff models. Predictions of ANN-based and multi-regression-based Gaussian puff models were compared with an ANN dispersion model, and Gaussian puff models using Slade's parametrizations and COMBIC (Combined Obscuration Model for Battlefield Induced Contaminants), a sophisticated Gaussian puff model with a number of enhancements to account for such additional effects as wind shear and ground interaction (Ayres and DeSutter 1995).

2 Field Experiments and Data Collection

The data used for ANN and multiple non-linear regression models of dispersion coefficients were the same as those we used for the direct ANN modelling of concentration dispersion (Cao et al. 2010). Briefly, data were collected during week-long trials conducted at Valcartier, Quebec, in all four seasons, on a 2 km^2 level plain. The surface was either covered with snow in the late autumn and winter trial periods (November and March), or sparsely covered with low grass in the spring (May) and summer (August). Puffs were released from an aerosol generator over a period of 2 s, with the aerosols used being polyvinyl chloride (PVC) microspheres (10^{-2} kg at a time, $d \approx 27\,\mu$m, 0.2×10^3 kg m^{-3}), glass spheres (2×10^{-2} kg at a time, $d \approx 6.5\,\mu$m) and talc powder (2×10^{-2} kg at a time). The generator exit port was 0.08 m in diameter, 0.5 m above the ground, at a 45° angle upward. The resulting clouds or puffs and their movement were scanned and detected using a lidar, a laser remote sensing system, located about 200 m from the release point and operated at 532 nm. At the same time, a meteorological system, located a few metres away from the lidar, regularly collected micrometeorological data, such as the three components of wind speed, wind direction, temperature and relative humidity at two heights, air pressure, insolation, ground heat flux and precipitation. The layout of the experimental instruments is shown in Fig. 1, where R_1 represents the position of the lidar, and D_1 to D_8 and SD_1 and SD_2 are puff release locations. The choice of the release location depended on the wind direction at the time. Details of the meteorological parameters measured, and the instrumentation used, can be found in Cao et al. (2010).

The scanning lidar was operated at a wavelength of 532 nm with a horizontal raster scanning pattern. The laser source emitted 12 ns pulses at a pulse repetition frequency of 100 Hz. The lidar scanned a volume spanned by a radial distance of about 450 m, a range of 82° in azimuth, and 10° in elevation. The radial resolution of the lidar scanning was 1.2 m, and its resolution in azimuth was about 0.8° and in elevation 0.5° or 1.0°, depending on the air stability. Under stable conditions, vertical cloud dispersion was small, and a 0.5° sweep interval was selected to measure more layers of the cloud, whilst under unstable conditions, with more vertical dispersion, a 1.0° sweep interval was used to scan the cloud from bottom to top. Each release was scanned six times, and each scan contained 6–10 sweeps on average. The measured signals were inverted into relative concentrations, proportional to their absolute concentrations, using a lidar inversion algorithm developed by the Defense Research and Development Canada (DRDC)-Valcartier lidar group (Bissonnette et al. 2003). More information on the lidar can be found in Cao et al. (2010).

Only those trials containing information on full clouds were used to derive distance variances in three major (downwind, crosswind and vertical) directions. Some 60 trials, containing 218 scans (with dispersion times less than 150 s) were selected. See Cao et al. (2010) for details of useful trial selection.

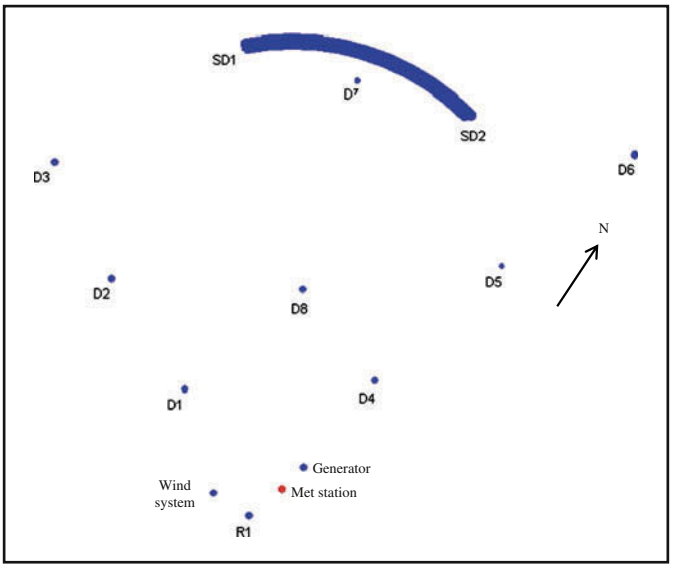

Fig. 1 Layout of measuring instruments

3 Dispersion Coefficients

Dispersion coefficients of an aerosol puff are functions of the initial puff size, dispersion time and turbulence (stability), and can be calculated using moments analysis. The moment for concentration, θ_{nmp}, is defined in terms of the concentration, $c(x, y, z, t)$, by the following relation:

$$\theta_{nmp}(t) = \int_{-\infty}^{+\infty}\int_{-\infty}^{+\infty}\int_{-\infty}^{+\infty} cx^n y^m z^p dxdydz, \tag{2}$$

for $m \geq 0$, $n \geq 0$, $p \geq 0$. In our study, a moving coordinate frame was used, with the centre of mass of a puff as the origin of the coordinate system. The dispersion coefficient in the x direction, σ_x, can be determined from the corresponding variance, σ_x^2, as the second moment:

$$\sigma_x^2(t) = \frac{\theta_{200}}{\theta_{000}} = \frac{\int_{-\infty}^{\infty}\int_{-\infty}^{\infty}\int_{-\infty}^{\infty} x^2 cdxdydz}{\int_{-\infty}^{\infty}\int_{-\infty}^{\infty}\int_{-\infty}^{\infty} cdxdydz}, \tag{3}$$

with similar expressions for σ_y and σ_z.

The downwind dispersion coefficient is a function of the initial size of the source puff, the turbulent portion, and the wind shear, and is usually expressed as

$$\sigma_x^2 = \sigma_{x0}^2 + \sigma_{xt}^2 + \sigma_{xs}^2, \tag{4}$$

where σ_{x0} is the dispersion coefficient of the source puff in the downwind direction, and σ_{xt} and σ_{xs} are terms reflecting the turbulent longitudinal diffusivity of the puff and the vertical wind shear, respectively (Draxler 1979). However, for the crosswind and vertical dispersion coefficients, the wind-shear effects can be ignored, so that only the source size and turbulent contributions need to be considered.

Table 1 Inputs for ANN models and data range

Inputs	Description	Range	
t	Dispersion time (s)	16.8	137.2
U	Mean transport wind speed ($\mathrm{m\,s^{-1}}$)	0.12	4.25
I	Solar irradiation ($\mathrm{W\,m^{-2}}$)	0.0	856.2
H	Ground heat flux ($\mathrm{W\,m^{-2}}$)	0.0	442.7
T	Temperature (°C)	−19.0	27.5
$\mathrm{d}T/\mathrm{d}z$	Temperature gradient, ($\mathrm{K\,m^{-1}}$)	−1.0	1.7
RH	Relative humidity (%)	27.5	98.2
p	Air pressure (kPa)	98.1	101.1

COMBIC uses Eq. 4 for downwind distances greater than the distance associated with a downwind travel time of 30 s, with σ_{xt} and σ_{xs} being functions of atmospheric stability (Pasquill stability category), scaling ratio (z/L, where L is the Obukhov length, and z is the height above the ground) and aerodynamic roughness length (z_0). When the downwind travel time is less than 30 s, a traditional power law is used, but with coefficients different from Slade's parametrizations (Ayres and DeSutter 1995).

In the ANN modelling of dispersion coefficients, since the first measured puff was used as the source, and the size of the first puff varied with turbulence, emphasis was put on the turbulent and wind-shear contributions, whilst the size of the source puff, σ_{i0}, was removed from the output, as shown in Eq. 5.

$$\sigma_i'^2 = \sigma_i^2 - \sigma_{i0}^2, \tag{5}$$

for $i = x, y, z$. For convenience, σ_i' is replaced by σ_i in the following unless specified otherwise.

4 ANN Modelling of Puff Dispersion Coefficients

We started examining neural networks with more inputs, including some preprocessed turbulence parameters, such as TKE (turbulent kinetic energy), Obukhov length, and the structure parameter for refractivity. However, adding these inputs did not provide much improvement, whilst making the ANN structure more complicated. Finally, we chose seven easily measurable meteorological variables (Table 1), along with the dispersion time, as inputs to the ANN models developed for puff dispersion coefficients.

The modelling process was the same as that used previously for aerosol concentration distributions (Cao et al. 2010). The output of the ANN is the concentration variance (square of the dispersion coefficient) without the initial size of the source puff. Since different dispersion coefficients are different functions of those inputs (atmospheric conditions and dispersion time), individual ANN models were developed for each dispersion coefficient σ_x, σ_y or σ_z.

The commercial shell used in this study was NeuralWorks Professional II/Plus from NeuralWare (2003). The particular paradigm used was a fully connected multi-layer feed forward (MLFF) back propagation (BP) network using the extended delta-bar-delta (EDBD) learning rule (Minai and Williams 1990), with each node in a given layer having a weight connecting it to every node in the next layer. For a network with one output node, the basic principle is that, at the start of the training process, the connecting weights throughout the network

are assigned random values, then each sample case is applied to the network, and the network produces an output based on the current state of its synaptic weights. The output value generated by the model is compared to the known corresponding measured output value. The difference between the predicted and known output (the global error) is propagated backwards through the network to change the weights of connections to reduce the error signal for the case in question. The cycle is repeated until the overall error value falls below some pre-determined threshold. Once the global error has been minimized over the whole training set, the weights are fixed and the network can be used to make blind predictions. Readers are referred to Patterson (1998) for more information on neural networks.

Artificial neural networks with one or more hidden layers were examined, and it was found that two or more hidden layers showed no obvious improvement in network performance. Consequently, a one-hidden-layer ANN was used. Further, it is difficult to determine the optimal number of hidden nodes, as this depends, in part, on the values of the connecting weights. During training, hidden nodes were successively removed until the simplest model (least number of hidden nodes) was developed that did not compromise performance, It should be pointed out that the nodes (and their connecting weights) are essentially fitting parameters, so it is felt that the fewer the number of hidden nodes, the more general the model.

4.1 Model Evaluation

Tens of ANN models were trained for each σ_i, $i = x, y, z$, where five models with the best performances were chosen, with each having 14–20 hidden nodes. Averages of the five best ANN model predictions were used, as the final prediction, under specified meteorological conditions. The developed ANN-based Gaussain puff models were evaluated, based on the following model performance measures: normalized mean square error ($NMSE$), fractional bias (FB), linear correlation coefficient (r), factor of two (F_2) and factor of 10 (F_{10}), where

$$NMSE = \frac{1}{N}\sum_i \frac{(P_i - M_i)^2}{\overline{P}\,\overline{M}} \tag{6}$$

$$FB = \frac{\overline{M} - \overline{P}}{0.5\left(\overline{M} + \overline{P}\right)} \tag{7}$$

and M_i is the measurement of σ_i, $i = x, y, z$, calculated from experimental data; P_i is the ANN prediction of σ_i, with an overbar indicating an average over the training or test set.

The perfect values for all those performance measures are:

$$NMSE = FB = 0,$$

and

$$r = F_2 = F_{10} = 1.$$

Table 2 is a summary of evaluations of the developed ANN models, based on the above performance measures. The ANN-based Gaussian puff model predictions are very close to the measurements, with correlation coefficients of 0.9, or even higher, for all three dispersion coefficients, and almost 100% of the predictions in the range of a factor of two. Small $NMSE$ and FB values also show the closeness of predictions to the measurements.

Table 2 Evaluation of ANN models for dispersion coefficients

	SET	$NMSE$	r	FB	F_2
σ_x	Training	0.056	0.928	−0.069	0.98
	Test	0.042	0.912	0.014	1.00
σ_y	Training	0.030	0.962	0.001	1.00
	Test	0.016	0.972	0.027	1.00
σ_z	Training	0.021	0.979	−0.007	1.00
	Test	0.033	0.975	−0.017	1.00

4.2 Model Comparison

The ANN-based Gaussian puff model and its normalized concentration predictions were compared with those from both Slade's Gaussian puff model and COMBIC, as well as the predictions from the direct ANN concentration dispersion model (Cao et al. 2010). Three validation sets under unstable, neutral and stable conditions were used.

As ANN models for dispersion coefficients only considered expansion from the initial size, the final expansion coefficients of the Gaussian puff model will be

$$\sigma_i^2(t) = \sigma_i^2(0) + \sigma_{ip}^2(t), \tag{8}$$

for $i = x, y, z$, where σ_{ip} is the average of σ_i predictions from the ANN models.

Since puffs were released near the ground, and the dispersion considered here was over a very short range (dispersion times less than 150 s after release), the dispersed puff was felt to be unlikely to reach to the top of the boundary layer. Therefore, only reflection from the ground needed to be considered, and the traditional Gaussian puff model, Eq. 1, was modified under the assumption of 100% ground reflection and no deposition, viz.

$$C(x, y, z, t) = \frac{Q}{(2\pi)^{3/2}\sigma_x\sigma_y\sigma_z} \exp\left\{-\frac{x^2}{2\sigma_x^2} - \frac{y^2}{2\sigma_y^2} - \left[\frac{(z-z_c)^2}{2\sigma_z^2} + \frac{(z+z_c)^2}{2\sigma_z^2}\right]\right\} \tag{9}$$

where z is the vertical distance above the ground, and z_c is the height of the centre of mass.

The direct ANN concentration dispersion model (Cao et al. 2010) generated predictions of normalized concentrations, i.e., concentrations normalized by the maximum concentration at the source. Consequently, for comparison purposes, all Gaussian puff models (ANN-based, Slade and COMBIC) predictions were also normalized by the source puff maximum concentration. Table 3 is a comparison of the performances of the ANN-based Gaussian puff model, the direct ANN puff dispersion model, Slade's Gaussian puff model and COMBIC for all measured cloud points. One can see from Table 3 that the direct ANN concentration distribution model gave the best predictions, with a greater portion being in the range of a factor of two, and having a lower *NMSE*, and the same or higher correlation coefficient. It should be noted that the use of this direct ANN model for concentration distributions should be restricted to the atmospheric conditions of the training data. The direct ANN concentration distribution model provided good predictions of concentrations near the centroid, but overestimated low concentrations. However, although the ANN-based Gaussian puff model may somewhat underestimate the highest concentrations, predictions for points away from the centroid are much better than the direct ANN predictions. When compared with the other

Table 3 Concentration prediction comparison from different models

Atmospheric stability	Model	*RMPE*	*NMSE*	*r*	*FB*	F_2	F_{10}
B Unstable	Puff_Multi_Regr	0.07	2.51	0.58	−0.01	0.42	0.87
	Gaussian_ANN	0.06	1.93	0.62	−0.17	0.39	0.86
	ANN	0.06	1.49	0.68	−0.45	0.43	0.85
	COMBIC	0.07	1.90	0.53	−0.44	0.34	0.81
	Slade's puff	0.08	8.34	0.48	0.82	0.36	0.93
E–D Neutral	Puff_Multi_Regr	0.08	6.19	0.66	1.11	0.24	0.73
	Gaussian_ANN	0.06	1.31	0.65	0.21	0.33	0.73
	ANN	0.08	1.16	0.64	−0.46	0.44	0.89
	COMBIC	0.06	1.14	0.66	−0.04	0.32	0.70
	Slade's puff	0.07	1.44	0.65	0.04	0.26	0.55
F Stable	Puff_Multi_Regr	0.05	0.62	0.69	−0.14	0.55	0.93
	Gaussian_ANN	0.06	0.87	0.63	−0.28	0.46	0.93
	ANN	0.06	0.79	0.66	−0.41	0.50	0.94
	COMBIC	0.13	2.10	0.67	−0.86	0.37	0.85
	Slade's puff	0.17	3.23	0.61	−0.87	0.31	0.84

two Gaussian-based puff models, the ANN-based puff model showed better performance in stable conditions (lower $NMSE$ and higher F_2).

Usually, the highest concentration of a puff is of the greatest concern. Table 4 lists the maximum measurements and predictions for each validation trial at different times. It shows that all three Gaussian puff models under-estimate the maximum concentrations to some extent. Also, predictions from the ANN-based Gaussian puff model and COMBIC in unstable conditions were close, though both underestimated the maximum concentration, especially when dispersion time was very short. Under stable conditions, predictions of the ANN-based puff model were closer to measurements than those from COMBIC, which were generally overestimated. It is only for the validation trial under neutral conditions that COMBIC was a little better than the ANN-based Gaussian puff model, when dispersion times were very short. Slade's Gaussian puff model greatly underestimated the maximum concentration in unstable conditions, and its performance in stable conditions was similar to that of COMBIC.

Based on the analysis above, it seems that a Gaussian puff model gives reasonable estimations for puff dispersion, so long as the dispersion coefficients are appropriately determined. For short dispersion times, the ANN-based Gaussian puff model was generally better than, or as good as, COMBIC and Slade's puff model.

5 Relationship Between Dispersion Coefficients and Dispersion Time

To check how dispersion coefficients change with time under different stability conditions, three atmospheric scenarios, representing unstable, stable and neutral conditions, were used for simulations. The dispersion time varied from 20 to 120 s, every 20 s, and wind speed varied for each case from 0.15 to 4.15 m s^{-1}, every 0.5 m s^{-1}. The Pasquill stability category was determined from the wind speed. Consequently, for the stable case at 0.15 m s^{-1}, its stability would change to neutral when wind speed increased to 4.15 m s^{-1}, and for the unstable case,

Table 4 Comparison of maximum normalized concentration predictions from Gaussian puff models using different dispersion coefficients (ANN-based, Slade, COMBIC and multi-regression)

Atmospheric stability	Time (s)	Max. meas.	Max. prediction			
			ANN-based Gaussian puff	Slade's puff	COMBIC	Multi-regr.
B Unstable	22.6	0.58	0.25	0.07	0.23	0.15
	42.7	0.28	0.08	0.02	0.11	0.07
	62.4	0.11	0.06	0.01	0.06	0.04
E–D Neutral	26.1	0.69	0.28	0.26	0.49	0.09
	49.2	0.39	0.23	0.13	0.31	0.04
	72.6	0.34	0.17	0.08	0.21	0.025
	96.1	0.31	0.13	0.05	0.15	0.02
	119.8	0.22	0.11	0.04	0.11	0.01
F Stable	17.9	0.46	0.37	0.68	0.68	0.27
	34.7	0.24	0.23	0.35	0.45	0.125
	50.1	0.14	0.19	0.37	0.37	0.094
	65	0.14	0.15	0.36	0.32	0.08

the stability changed from very unstable to slightly unstable when wind speed increased from 0.15 to 4.15 m s^{-1}. The determination of the Pasquill stability followed the scheme used in COMBIC (Ayres and DeSutter 1995).

Figure 2 shows the dispersion coefficients generated by the ANN model as functions of time and wind speed in stable (Fig. 2a), neutral (Fig. 2b) and unstable (Fig. 2c) conditions. Dispersion coefficients σ_x, σ_y and σ_z are represented by circles, triangles and squares, respectively, with the related regressions also shown in Fig. 2. Since most of the training data available in unstable and neutral conditions are for dispersion times less than 80 s, only predictions for times less than 80 s were used for the regressions.

The simulation result for σ_z was complicated, since puff size was seen to increase with time from 20 to 40 s, but then decrease somewhat under stable conditions. Intuitively, it is inconceivable that the puff would decrease in size with time, unless an increasing number of cloud points away from the centroid became well mixed with the background atmosphere and thus were not be able to be detected (although this was not felt to be the case here). A possible explanation is that, as the lidar scanned the puff, slice by slice, part of the cloud bottom or top might be missed. A missing portion would probably have little influence on the value of σ_z under neutral and unstable conditions, because of the relatively large values involved. However, the influence of a missing cloud portion under stable conditions may play a bigger role in σ_z than under other conditions, and might result in smaller puffs being sensed. This phenomenon was, in fact, observed in some of the releases in stable conditions. It is felt, though, that the amount lost was small, so it is reasonable to assume that, for short dispersion times, vertical dispersion coefficients would increase with time. As a result, power-law regressions were felt to be good fits in stable conditions. For neutral and unstable conditions, as stated before, only predictions shorter than 80 s were considered for analysis, and here again, power-law regressions provided good approximations. Figure 2 also shows that $\sigma_x > \sigma_y > \sigma_z$ in stable and neutral conditions, although in unstable conditions, $\sigma_z > \sigma_y > \sigma_x$ for short dispersion times.

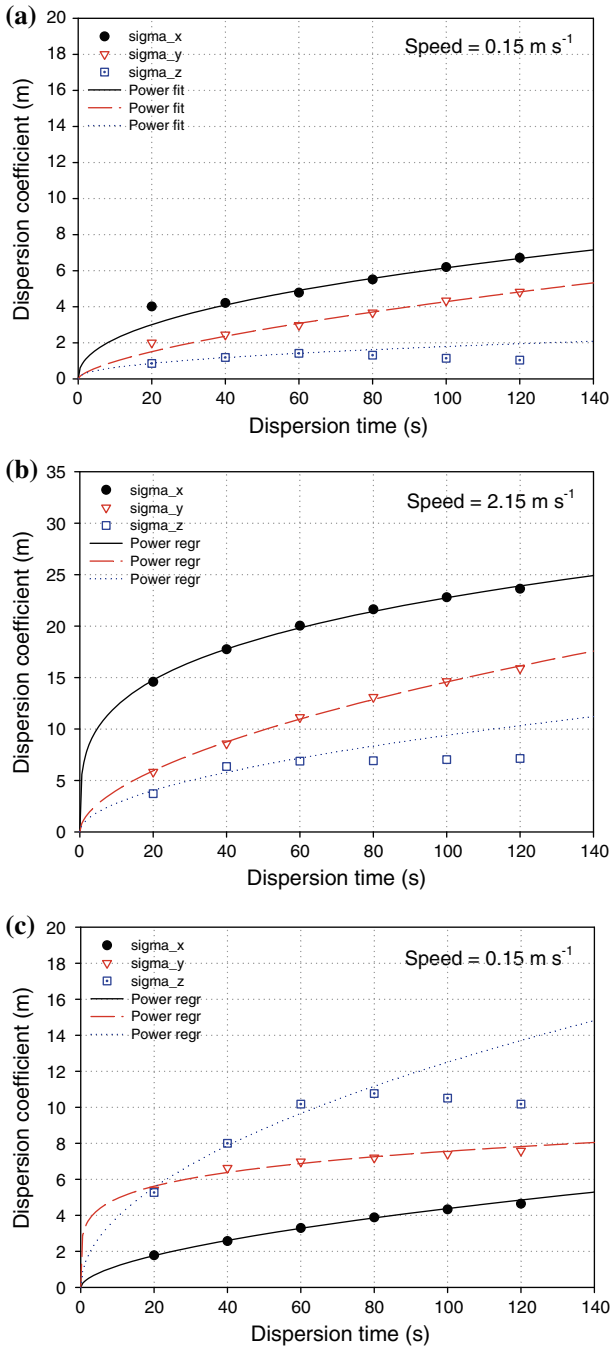

Fig. 2 ANN predicted dispersion coefficient changes with dispersion time, with the corresponding Pasquill stability indicated as: **a** stable, **b** neutral, **c** unstable

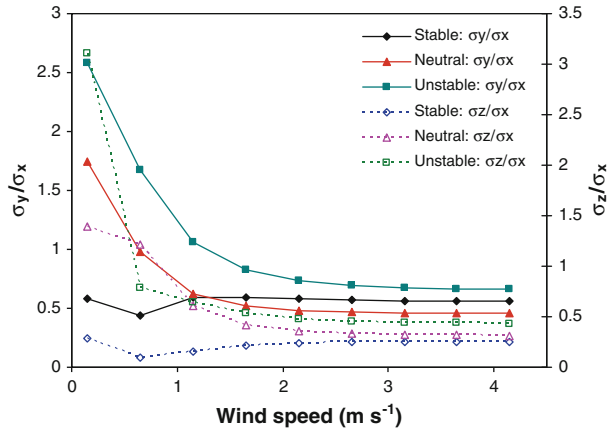

Fig. 3 Gaussian puff shape (σ_y/σ_x, σ_z/σ_x) change with wind speed for simulated cases

As empirical models, ANN models are generally valid when the deployment conditions are within the ranges used in model development, especially for dispersion time. However, since atmospheric conditions represent stability of the atmosphere, and the training data covered all possible Pasquill stability conditions, as long as the stability does not change dramatically, even if the atmospheric condition is slightly outside of the training set, the predictions should still be reasonably good. Examples are shown in Fig. 3, which shows that the ANN model's predictions of dispersion coefficients change with wind speed, for each simulated case. For the stable case, when wind speed increases, the stability changes from stable to near-neutral conditions, the cloud/puff shape increases initially with wind speed, then changes little when wind speed increases further and the stability is near neutral. For the unstable case, when the wind speed is $0.15\,\mathrm{m\,s^{-1}}$, conditions are very unstable, and the cloud undergoes significant dispersion (large σ_y/σ_x and σ_z/σ_x). When wind speed increases, the stability changes to slightly unstable, then further to near neutral. The cloud shape reduces as stability increases. From Fig. 3, it seems the ANN models are capable of providing reasonably good predictions, even when wind speed further increases over the wind limit of the training set. We believe that, so long as the dispersion time is within the training set or not far from restrictions of the training data, the ANN models will provide good predictions of dispersion coefficients for Gaussian puff models.

Since the output function of an ANN model is a function of all of the inputs and hidden layer nodes, and we used the average of five ANN models that have different numbers of hidden nodes, it is difficult to extract functional relationships between the output and each individual input. An ideal model is one providing reasonable predictions, with a simple structure, whilst clearly explaining the influence of each input on the output. Non-linear multi-variable regressions provide one way of achieving this goal.

6 Multi-Variable Non-linear Regression Model of Dispersion Coefficients

Slade's power law for Gaussian puff dispersion coefficients (along with other models) was based on discrete Pasquill stability categories. Since each category covers a fairly broad range of constituent atmospheric parameters, these models are somewhat insensitive to changes in

Table 5 Parameters of non-linear multiple variable regression functions for dispersion coefficients

	Function	$c(U)$	$c(H)$	$c(T)$	$c(\mathrm{d}T/\mathrm{d}z)$	$c(P)$	$c(RH)$	$c(TKE)$
σ_x	f_1	0.7928	−0.1838	0.5514	0.5772	0.6336	−1.0786	0.0818
	f_2	−0.2848	0.1171	−0.3293	−0.2573	−0.4015	0.5297	−0.0083
σ_y	f_1	1.2463	0.2505	0.2946	0.2423	−0.4601	0.5645	−0.2252
	f_2	−0.3923	−0.1212	−0.0812	−0.1219	0.1782	−0.3824	0.0809
σ_z	f_1	0.1058	−0.1614	−0.0464	0.2088	1.7469	−2.4836	−0.1545
	f_2	0.0666	0.1519	0.3166	−0.1235	−1.5185	1.6314	0.2117

atmospheric conditions. In addition, it is often unclear which Pasquill stability category should be used for conditions near the limits or transition between categories. Here, we are developing models using atmospheric measurements explicitly, so that no predetermination of discrete stability categories is necessary.

Further, a sensitivity analysis of ANN models for dispersion coefficients showed that insolation had little influence on any of the three dispersion coefficients, so this parameter was excluded from the inputs considered in the non-linear multi-regression. The general power regression is shown as:

$$\sigma_i = k_1 t^{k_2}, \tag{10}$$

for $i = x, y, z$ where both k_1 and k_2 are functions of atmospheric conditions, mean wind speed (U), ground heat flux (H), air temperature (T), air temperature gradient $(\mathrm{d}T/\mathrm{d}z)$, air pressure (p), relative humidity (RH) and turbulent kinetic energy *(TKE)*, with these parameters being used to represent the air stability conditions, i.e.,

$$k_j = f_j(U, H, T, \mathrm{d}T/\mathrm{d}z, p, RH, TKE), \tag{11}$$

for $j = 1, 2$. To develop a non-linear multiple variable regression, a function has to be pre-specified. A power function is usually robust and is employed here, such that

$$f_j = U^{c_{j1}} H^{c_{j2}} T^{c_{j3}} (TR)^{c_{j4}} p^{c_{j5}} (RH)^{c_{j6}} (TKE)^{c_{j7}}, \tag{12}$$

for $j = 1, 2$; Table 5 lists the coefficients of c_{jk} for function f_1 and f_2.

The coefficients listed in Table 5 were applied to simulation trials and the results were assessed based on the same evaluation measures, or metrics, and shown in Table 3 for comparison with other models. It was found that Gaussian puff predictions based on dispersion coefficients from non-linear multiple variable regressions are better than other models for moderately stable and unstable conditions, whilst under neutral conditions, concentration predictions are usually lower than observations.

However, it was also found that predictions of maximum normalized concentrations from multiple variable regressions are lower than other models, as seen in Table 4. The relatively high correlation coefficient was due to the great number of low concentration predictions, which were somewhat better than those of the other models.

7 Conclusion and Discussion

Puff dispersion can be characterized effectively by simple Gaussian puff models, if proper dispersion coefficients are provided and the centroid of the puff can be derived. The ANN

model developed for puff dispersion coefficients was based on field experimental data covering a wide range of meteorological conditions. The model used the meteorological parameters as direct inputs that can be easily measured, and avoided predefining the Pasquill stability category, as must be done for most existing models. To the best of our knowledge, this is the first time neural networks have been used to determine dispersion coefficients for Gaussian puff models, and the predicted results were generally better than, or as good as, other Gaussian models (COMBIC and Slade's puff model).

The limitation in using ANN models to estimate dispersion coefficients is that these models are only valid within the data range used in model development. Predictions for conditions outside the training range, especially for dispersion time, require extrapolation, a weakness of any empirical correlation. However, based on simulation results, it was found that, as long as the atmospheric condition is not too far from the training data, then the ANN models can still provide reasonably good predictions for dispersion coefficients.

Non-linear multiple variable regressions were also developed from the same trial data, with predictions from these being close to, or even somewhat better than, those of the ANN-based Gaussian puff model. The predictions were particularly close to measured values for the large number of low concentration points, whilst tending to underestimate maximum concentrations.

Our future plans are to integrate the developed direct ANN model for concentration dispersion and the ANN-based Gaussian puff model with either optimization or Bayesian inference to address source detection. This is usually turned into an optimization problem (Allen et al. 2007; Cervone et al. 2010) or using Bayesian inference methods (Keats et al. 2007; Senocak et al. 2008), along with a proper forward dispersion model. Both the direct ANN model for concentration distribution (Cao et al. 2010), or the ANN models for dispersion coefficients of Gaussian models proposed herein, can be used as the forward dispersion model. Since the proposed ANN models predicting the dispersion coefficients are based on real-time atmospheric conditions and dispersion time, when a source location is known or assumed, then the dispersion time can be derived based on the distance to the source. Alternatively, if cloud dimensions can be determined, either partially or completely, these dimensions can be used to determine the corresponding dispersion coefficients. Based on the current meteorological condition, the dispersion coefficients are functions of x or t. These, in turn, can be used to determine the upwind location of the source.

Acknowledgments The authors wish to express appreciation for the financial support of the Natural Sciences and Engineering Research Council of Canada, the Academic Research Program of the Royal Military College of Canada, Director General Nuclear Safety and the CBRN Research and Technology Initiative of the Canadian Department of National Defence. Numerous colleagues at Defence Research and Development Canada Valcartier assisted with the data collection. To all these people, we are extremely grateful.

References

Allen CT, Young GS, Haupt SE (2007) Improving pollutant source characterization by better estimating wind direction with a genetic algorithm. Atmos Environ 41:2283–2289

Arya SP (1999) Air pollution meteorology and dispersion. Oxford University Press, New York 310

Ayres SD, DeSutter S (1995) Combined Obscuration Model for Battlefield Induced Contaminants (COMBIC92) model documentation. U.S. Army Research Laboratory, Battlefield Environment Directorate, White Sands Missile Range, NM 88002-5501, 251 pp

Bissonnette LR, Roy G, Vallee G, Cantin S (2003) Mesures lidar d'un panache d'insecticide émanant d'une source continue. RDDC Valcartier ECR 2003–273, 32 pp

Cao X, Roy G, Andrews WS (2010) Modelling the concentration distributions of aerosol puffs using artificial neural networks. Boundary-Layer Meteorol 136(1):83–103

Cervone G, Franzese P, Keesee AP (2010) Algorithm quasi-optimal (AQ) learning. WIREs Comput Stat 2(2):218–236
Chatwin PC (1968) The dispersion of a puff of passive contaminant in the constant stress region. Q J Roy Meteorol Soc 94:350–360
De Haan P (1999) On the use of density kernels for concentration estimates within particle and puff dispersion models. Atmos Environ 33:2007–2021
De Hann P, Rotach MW (1998) A novel approach to atmospheric dispersion modelling: the Puff-Particle Model. Q J Roy Meteorol Soc 124:2771–2792
DeVito TJ, Cao X, Roy G, Costa JR, Andrews WS (2009) Modelling aerosol concentration distributions from transient (puff) sources. Can J Civ Eng 36(5):911–922
Draxler RR (1979) Some observations of the along-wind dispersion parameter. In: 4th Symposium on Turbulence, diffusion, and air pollution of the American Meteorological Society, Reno, NV. Preprint, January 15–18, 1979, pp 5–8
Islitzer NF, Slade DH (1968) Diffusion and transport experiments. In: Slade DH (ed) Meteorology and atomic energy. TID-24190. USAEC, Springfield, pp 163–175
Keats A, Yee E, Lien F (2007) Bayesian inference for source determination with applications to a complex urban environment. Atmos Environ 41:465–479
Minai AA, Williams RD (1990) Acceleration of back-propagation through learning rate and momentum adaptation. In: Proceedings of the IEEE/INNS international joint conference on Neural Networks-90-WASH-DC, Washington, DC, vol 1, pp 676–679
NeuralWare (2003) Reference guide: NeuralWorks Professional II/Plus and NeuralWorks Explorer, Pittsburgh, PA, 283 pp
Pasquill F, Smith FB (1983) Atmospheric diffusion, 3rd edn. Wiley, Chichester, 297 pp
Patterson DW (1998) Artificial neural networks: theory and applications. Simon and Schuster, New York, 400 pp
Sato J (1995) An analytical study on longitudinal diffusion in the atmospheric boundary layer. Geophys Mag Ser 2 1(2):105–151
Senocak I, Hengartner N, Short M, Daniel W (2008) Stochastic event reconstruction of atmospheric contaminant dispersion using Bayesian inference. Atmos Environ 42:7718–7727
Turner DB (1994) Workbook of atmospheric dispersion estimates–an introduction to dispersion modelling, 2nd edn. CRC, Boca Raton, 192 pp
Van Ulden AP (1992) A surface-layer similarity model for the dispersion of a skewed passive puff near the ground. Atmos Environ 26A(4):681–692
Wilson DJ (1981) Along-wind diffusion of source transients. Atmos Environ 15(4):489–495
Wilson JD, Sawford BL (1996) Review of Lagrangian stochastic models for trajectories in the turbulent atmosphere. Boundary-Layer Meteorol 78:191–210